

## Phenol Electrooxidation in Different Supporting Electrolytes Using Boron-Doped Diamond Anodes

Renata Beraldo Alencar de Souza and Luís Augusto Martins Ruotolo\*

Department of Chemical Engineering, Federal University of São Carlos, P.O. Box 676 13565-905 São Carlos-SP, Brazil

\*E-mail: [pluis@ufscar.br](mailto:pluis@ufscar.br)

Received: 25 October 2012 / Accepted: 2 December 2012 / Published: 1 January 2013

---

In this work phenol was used as a model compound to study the influence of supporting electrolytes on the electrochemical oxidation of organic pollutants in aqueous medium, in absence and presence of chloride anions. The experiments were carried out in a flow electrochemical reactor using a boron-doped diamond (BDD) anode. The kinetics of chemical oxygen demand removal followed the pseudo-first order model, indicating that the process was mass transfer controlled. The supporting electrolytes containing nitrate and phosphate exhibited kinetics slower than those obtained using sulfate and carbonate. The addition of chloride greatly increases the process kinetics, especially at the very low pH provided by H<sub>2</sub>SO<sub>4</sub> solutions. It was found that the electrooxidation kinetics, current efficiency and energy consumption are much more sensitive to the presence of chloride and the formation of oxidative chloro species than to supporting electrolytes through the formation of peroxysulfates or peroxycarbonates in the cases where sulfate and carbonate electrolytes were used.

---

**Keywords:** diamond electrodes; electrooxidation; supporting electrolytes; flow reactor; effluent treatment

### 1. INTRODUCTION

Phenol and many phenolic compounds present in industrial wastewaters are known to be recalcitrant to biological treatment and need to be eliminated by physical-chemical methods in order to be discharged according to the environmental regulatory laws [1]. Moreover, effluents containing phenolic compounds are produced by a large variety of industries. Among the physical-chemical technologies, the electrochemical method has been intensively studied due to its advantages such as reduction of workmanship due to easy automatization and environmental compatibility, since the main reaction reagent is the electron [2,3]. However, the main drawback that must be overcome in order to make the electrochemical treatment attractive for an effective industrial application is its high energy

consumption, which could be reduced by using electrodes with high oxygen evolution potential and mediated oxidation.

Phenol also has been used as a model compound in order to evaluate the oxidation power of several types of electrodes, such as doped SnO<sub>2</sub>, PbO<sub>2</sub>, DSA<sup>®</sup>, and boron doped diamond [4-7]. Among these electrodes, BDD showed the best results in terms of oxidation kinetics due to its unique characteristic of forming hydroxyl radicals weakly adsorbed, which promotes the fast and efficient reaction with organic molecules [8]. However, when the concentration becomes very low, mass transfer limitations make the current efficiency very small. Considering the very short life time of <sup>•</sup>OH radical, its reaction with organic molecules can only occur adjacent to electrode surface. In this situation, one strategy commonly used to improve the oxidation rate is to add anions, generally chloride, which can also be further oxidized and will serve as a mediator in the organic oxidation [9,10]. In the case of chloride, different chloro oxidant species can be formed, depending on the solution pH [11]. At low pH, chloride is oxidized at anode surface to form chlorine gas, which can remain dissolved in the aqueous solution according to equation (1)



At the cathode surface water reduction occurs



Chlorine can also be hydrolyzed forming hypochlorous acid according to equation (3). This reaction is irreversible for pHs greater than 3 and reversible for pHs lower than 3 (equation (4)).



For neutral and high pH, hypochlorite will be the predominant specie:



The chloro species can also react themselves (equation (6)) or with the hydroxyl radicals, to form more oxidized species (equations (7) and (8)), or even can be directly oxidized on the electrode surface (equation (9)), mainly forming chlorate and perchlorate [12].





BDD, due to its high OER overpotential, has been also used to generate other stable oxidants. The type of oxidant to be formed depends on the supporting electrolyte used. In general, these oxidants are stable and generated by a sequence of chemical and electrochemical steps. For example, in the case of a supporting electrolyte containing phosphate anions, Cañizares *et al.* [13,14] verified that initially peroxyphosphate is formed and then they combines themselves to generate the peroxydiphosphate anions, according to reactions 10 and 11.



Another powerful oxidant that has been cited by several authors is the peroxydisulfate, formed in sulfate-containing electrolytes, according to equations (12) and (13) [15-18].



Another oxidant that can be formed using carbonate solutions at very high potential on BDD electrodes is the peroxy carbonate [19]. Initially, carbonate dissociates according to equation (14), forming  $\text{HCO}_3^-$ , which is then oxidized to peroxy carbonate through the reaction with hydroxyl radicals (equation (15)).



Considering that many industrial effluents containing organics have low conductivity, a supporting electrolyte must be added not only to increase their conductivity, but mainly to reduce the cell potential in order to make the electrochemical process feasible in terms of energy consumption. The choice of the supporting electrolyte should take into account not only the conductivity, but also the possibility of they give a further contribution to the electrooxidation process through the formation of oxidant mediators, as previously discussed. Hence, current efficiency and energy consumption could be improved.

In this work, we studied and compared the effect of different types of supporting electrolytes and their concentration on the kinetics of phenol oxidation using a BDD electrode. The electrochemical process was followed by measuring the chemical oxygen demand (COD) and total phenolic compound (TPC) depletion along the electrolysis time. The kinetics, current efficiency, and energy consumption were determined for the different experimental conditions. Although some

authors have studied the effect of supporting electrolytes on electrochemical oxidation, in this work we provide a comparison of different supporting electrolytes in the presence and absence of chloride ions and a discussion of their practical influence on the electrooxidation process from the point of view of average current efficiency and energy consumption.

## 2. EXPERIMENTAL

Phenol (Aldrich) solutions were prepared using deionized water and an initial concentration of 280 mg L<sup>-1</sup>, which corresponds to 666 mg L<sup>-1</sup> COD. Phenol was chosen because it is currently used as a model compound to evaluate electrochemical oxidation.

Different supporting electrolytes were added to phenol solutions at different concentrations, maintaining the same ionic strength (I) in all experiments. The supporting electrolytes studied were H<sub>3</sub>PO<sub>4</sub> (Mallinckrodt), HNO<sub>3</sub> (Qhemis), H<sub>2</sub>SO<sub>4</sub> (JT Baker), NaNO<sub>3</sub> (Synth), Na<sub>2</sub>CO<sub>3</sub> (Synth), and Na<sub>2</sub>SO<sub>4</sub> (Synth). The effect of chloride was also studied by adding NaCl to obtain solutions with 200 mg L<sup>-1</sup> and 700 mg L<sup>-1</sup> Cl<sup>-</sup>. All chemicals were of analytical grade. The electrolyte volume used in all experiments was 1.5 L.

Voltammeteries of all supporting electrolytes in absence and presence of phenol were recorded using a PGSTAT 30 Autolab potentiostat. All potentials reported were measured using an Ag/AgCl reference electrode.

The electrolyses were performed in a flow reactor applying a constant flow velocity (0.32 m s<sup>-1</sup>). The gap between work and counter electrodes was 5.0 mm. A 4.0 cm x 7.0 cm 4500 ppm boron-doped diamond purchased from EUT GmbH (Einlenburg, Germany) was used as anode. A 5 μm BDD thickness (+/- 10% homogeneity) deposited on 2.0 mm niobium substrate, giving a total ohmic resistance of 20 mΩ cm, was used in all experiments. The counter electrode was a stainless steel plate with the same geometric area as the anode. The experiments were carried out under galvanostatic condition applying 50 mA cm<sup>-2</sup>. Electrolyte circulation between reservoir and reactor was done using a centrifugal pump. The electrolyte temperature was maintained in the range of 27-30 °C by a thermostatic bath.

Electrolyte samples were collected during the electrolysis for COD measurement by the standardized colorimetric technique using dichromate (Hach, Germany) and TPC concentration using the Folin-Ciocalteu method [20]. The values of TPC were expressed in mg L<sup>-1</sup> of gallic acid, which is the standard phenolic compound commonly used. Cell voltage was also measured and used to calculate the energy consumption. UV spectrophotometric measurements of electrolyte samples were recorded using an Amersham Pharmacia UV-Vis spectrophotometer.

The electrooxidation process was evaluated in terms of average current efficiency (ACE) and average energy consumption (AEC), calculated according to equations (16) and (17), respectively.

$$ACE = \frac{F \cdot V}{8 \cdot i \cdot A} \frac{\int_0^t \left( \frac{dCOD}{dt} \right) dt}{\int_0^t dt} \quad (16)$$

$$AEC = \frac{E_{cell} \cdot i \cdot A}{V \frac{\int_0^t (dCOD/dt) dt}{\int_0^t dt}} \quad (17)$$

In these equations,  $V_s$  is the electrolyte volume,  $F$  Faraday constant,  $i$  current density,  $A$  electrode area,  $t$  electrolysis time, and  $E_{cell}$  cell potential. The integration limits were established considering the time necessary to remove 80% of the initial COD.

### 3. RESULTS AND DISCUSSION

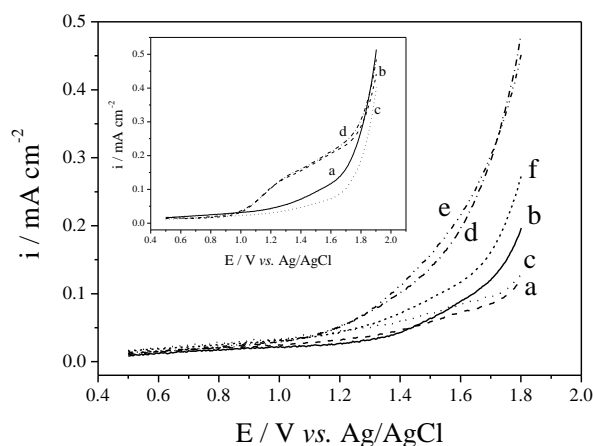


**Figure 1.** Voltammograms for BDD in absence of phenol and  $I = 0.3 \text{ mol L}^{-1}$ : a)  $\text{H}_3\text{PO}_4$ , b)  $\text{HNO}_3$ , c)  $\text{H}_2\text{SO}_4$ ; d)  $\text{Na}_2\text{CO}_3$ , e)  $\text{NaNO}_3$ , and f)  $\text{Na}_2\text{SO}_4$ . Inset: voltammograms for  $\text{Na}_2\text{SO}_4$ ,  $I = 0.3 \text{ mol L}^{-1}$  (curves a and b) and  $I = 3.0 \text{ mol L}^{-1}$  (curves c and d), in absence (curves a and c) and presence (curves b and d) of  $1.0 \text{ g L}^{-1}$  phenol.

It has been recognized that many anions can be further oxidized through the reaction with hydroxyl radicals generated on BDD electrodes at high anodic overpotentials, *e.g.*  $\text{PO}_4^{2-}$ ,  $\text{CO}_3^{2-}$ , and  $\text{SO}_4^{2-}$  can be oxidized to peroxodiphosphate [15], peroxysulfate [21], and peroxycarbonate [19], respectively. It has been also recognized that these anions improve the oxidation of organic molecules since they are strong oxidants. On the other hand, many industrial effluents would require the addition of supporting electrolytes in order to make them conductive and suitable for an electrochemical treatment. Therefore, the best supporting electrolyte would be one that is able to provide high conductivity (low cell potentials) and fast reaction kinetics for organic degradation, consequently energy consumption would be drastically reduced.

In order to verify how different supporting electrolytes affect the electrochemistry of the oxygen evolution reaction (OER) and phenol oxidation, Figure 1 shows the voltammograms for the BDD electrode in the absence and presence of phenol. It is interesting to notice that acidic electrolytes

displace the OER potential to more positive values and promote the suppression of the OER, as well. When phenol is added (inset of Figure 1), a peak corresponding to phenol oxidation starts at  $\sim 1.0$  V for  $\text{Na}_2\text{SO}_4$  like other electrolytes (not shown). Voltammograms of  $\text{Na}_2\text{SO}_4$  (inset of Figure 1),  $\text{H}_2\text{SO}_4$  and  $\text{Na}_2\text{CO}_3$  (not shown) with an ionic strength of  $3.0 \text{ mol L}^{-1}$  show that for the electrolytes containing  $\text{SO}_4^{2-}$  there is an inhibition of OER, while for  $\text{Na}_2\text{CO}_3$ , the increase of the ionic strength causes a huge increase of OER.

### 3.1. Phenol oxidation in the absence of chloride ions.

Figure 2 shows the normalized COD depletion against time. In all cases, the kinetics of COD removal followed a pseudo-first order model, indicating mass transfer control. The pseudo-first-order kinetic constants ( $k$ ) were determined with exponential regression and least square method. The correlation coefficients were greater than 0.98 in all cases. The following sequence was obtained:  $k_{\text{Na}_2\text{SO}_4}$  ( $0.488 \text{ h}^{-1}$ )  $\approx k_{\text{Na}_2\text{CO}_3}$  ( $0.486 \text{ h}^{-1}$ )  $> k_{\text{H}_2\text{SO}_4}$  ( $0.461 \text{ h}^{-1}$ )  $> k_{\text{H}_3\text{PO}_4}$  ( $0.378 \text{ h}^{-1}$ )  $> k_{\text{NaNO}_3}$  ( $0.314 \text{ h}^{-1}$ ), indicating that the supporting electrolytes have an influence on the oxidation kinetics, especially for those containing sulfate due to the strong oxidizing power of persulfate [22].

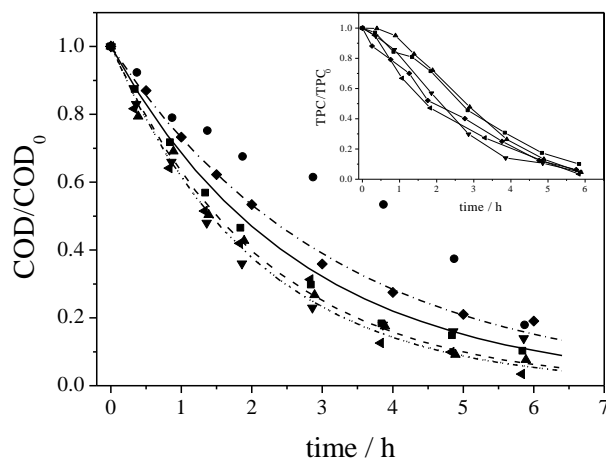


**Figure 2.** Normalized COD against time.  $\blacksquare$   $\text{H}_3\text{PO}_4$ ,  $\bullet$   $\text{HNO}_3$ ,  $\blacktriangle$   $\text{H}_2\text{SO}_4$ ;  $\blacktriangledown$   $\text{Na}_2\text{CO}_3$ ,  $\blacklozenge$   $\text{NaNO}_3$ ,  $\blacktriangleleft$   $\text{Na}_2\text{SO}_4$ .  $I = 0.3 \text{ mol L}^{-1}$ . Lines represent the fitted exponential model for  $\text{H}_3\text{PO}_4$  (—),  $\text{H}_2\text{SO}_4$  (- - -),  $\text{Na}_2\text{CO}_3$  (·····),  $\text{NaNO}_3$  (-·-·-·-), and  $\text{Na}_2\text{SO}_4$  (-·-·-·-·-). Inset: normalized TPC against time.  $\text{COD}_0 = 666 \text{ mg L}^{-1}$  ( $280 \text{ mg L}^{-1}$  phenol),  $\text{TPC}_0 = 30 \text{ mg L}^{-1}$  gallic acid.

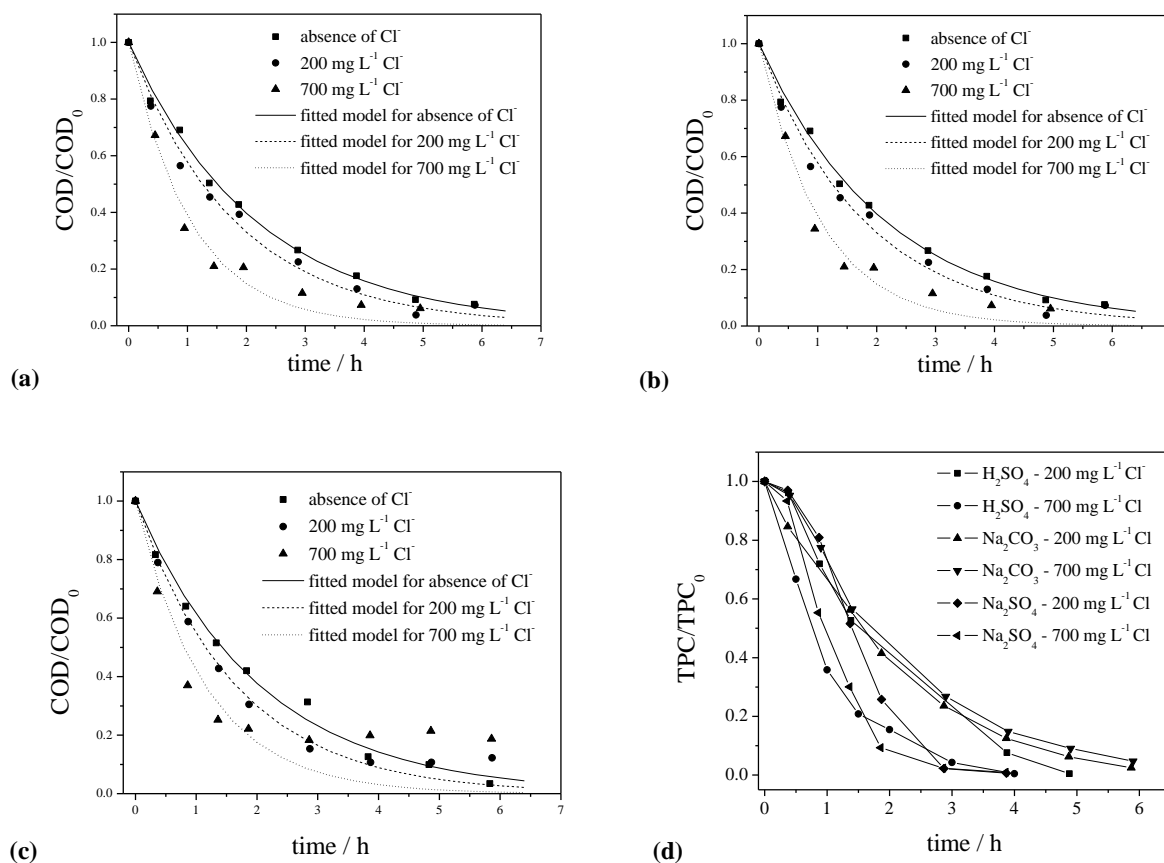
Moreover, according to the voltammograms shown in Figure 1, the sulfate-containing electrolytes also suppress the OER current. However, it is interesting to notice that even with high currents for OER observed in Figure 1 for  $\text{Na}_2\text{CO}_3$  electrolyte, it also exhibited an oxidation kinetics comparable to that obtained using  $\text{Na}_2\text{SO}_4$ . Actually, when phenol is added to the electrolyte, the voltammograms for  $\text{Na}_2\text{SO}_4$  and  $\text{Na}_2\text{CO}_3$  (not shown) were quite similar.

The least effective electrolyte was  $\text{NO}_3^-$ . The COD-time curve obtained using  $\text{HNO}_3$  did not follow the same kinetics as the others and a yellowish solution was observed, which could be attributed

to refractory intermediates formed during the electrochemical oxidation, such as branched nitrated phenols [23] or nitrate reduction to nitrite in acid electrolyte, as reported by Li *et al.* [24]. Regarding to the use of  $\text{H}_3\text{PO}_4$  as a supporting electrolyte, although the results for phenol oxidation were not bad, the process kinetics was slower than those obtained using sulfuric acid, sodium sulfate, and sodium carbonate. Additionally, the high cost of this acid compared to the other chemicals would not justify its use as supporting electrolyte. Considering all of these aspects, nitrate and phosphate electrolytes were not used for further experiments.

The inset of Figure 2 shows the degradation kinetics of phenolic compounds. It can be verified that using acid electrolytes the reaction rates are slower than those obtained using salt electrolytes. These results indicate that the aromatic ring is more difficult to be oxidized at low pH than at neutral pH (salt electrolytes). Although there is a difference in the kinetics of TPC removal during the three first hours of electrolysis, after six hours practically all TPC was removed, despite of the supporting electrolyte used.

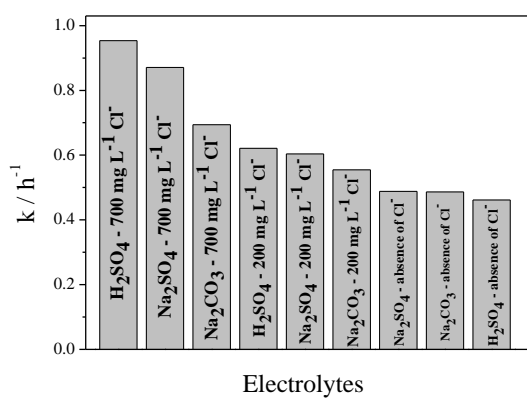
### 3.2. Phenol oxidation in the presence of chloride



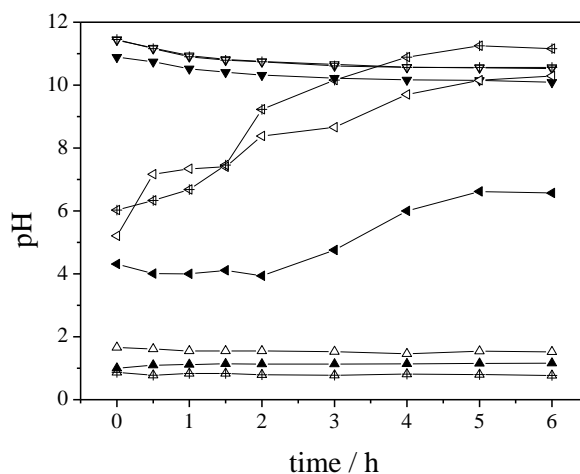
**Figure 3.** Normalized COD (a, b and c) and TPC (d) against time in absence (■) and presence of 200 mg L<sup>-1</sup> (●) and 700 mg L<sup>-1</sup> (▲) of chloride. Supporting electrolytes: (a) H<sub>2</sub>SO<sub>4</sub>, (b) Na<sub>2</sub>CO<sub>3</sub>, and (c) Na<sub>2</sub>SO<sub>4</sub>.  $I = 0.3 \text{ mol L}^{-1}$ . Lines represent the fitted exponential model for experiments carried out in absence (—) and presence of 200 mg L<sup>-1</sup> (- - -) and 700 mg L<sup>-1</sup> (·····) of Cl<sup>-</sup>. COD<sub>0</sub> = 666 mg L<sup>-1</sup> (280 mg L<sup>-1</sup> phenol), TPC<sub>0</sub> = 30 mg L<sup>-1</sup> gallic acid.

Figure 3(a)-(c) shows the normalized COD concentration against electrolysis time for the different electrolytes investigated. It can be seen that in all cases the process was mass transfer controlled as indicated by the exponential-shape of these curves. It can also be observed an important kinetics enhancement when chloride ions are added to the electrolyte.

The pseudo-first order kinetics constants were determined by exponential regression of the concentration-time data using the Levenberg-Marquadt estimation method. The results are shown in Figure 4, in which it is possible to observe that although the type of supporting electrolyte have influence on reaction kinetics, the influence of chloride ions is more important, especially at the concentration of 700 mg L<sup>-1</sup> Cl<sup>-</sup>. According to Figure 4, the best reaction rates are obtained in acidic medium, indicating that the pH is playing an important role on the oxidation process, especially in the presence of chloride.



**Figure 4.** Pseudo-first order kinetics constants for the experiments carried out using different supporting electrolytes in absence and presence of chloride.



**Figure 5.** pH against time: ▲ H<sub>2</sub>SO<sub>4</sub> in absence of Cl<sup>-</sup>; △ H<sub>2</sub>SO<sub>4</sub> + 200 mg L<sup>-1</sup> Cl<sup>-</sup>; ♣ H<sub>2</sub>SO<sub>4</sub> + 700 mg L<sup>-1</sup> Cl<sup>-</sup>; ▼ Na<sub>2</sub>CO<sub>3</sub> in absence of Cl<sup>-</sup>; ▽ Na<sub>2</sub>CO<sub>3</sub> + 200 mg L<sup>-1</sup> Cl<sup>-</sup>; ⦿ Na<sub>2</sub>CO<sub>3</sub> + 700 mg L<sup>-1</sup> Cl<sup>-</sup>; ◀ Na<sub>2</sub>SO<sub>4</sub> in absence of Cl<sup>-</sup>; ◁ Na<sub>2</sub>SO<sub>4</sub> + 200 mg L<sup>-1</sup> Cl<sup>-</sup>; ⦿ Na<sub>2</sub>SO<sub>4</sub> + 700 mg L<sup>-1</sup> Cl<sup>-</sup>.

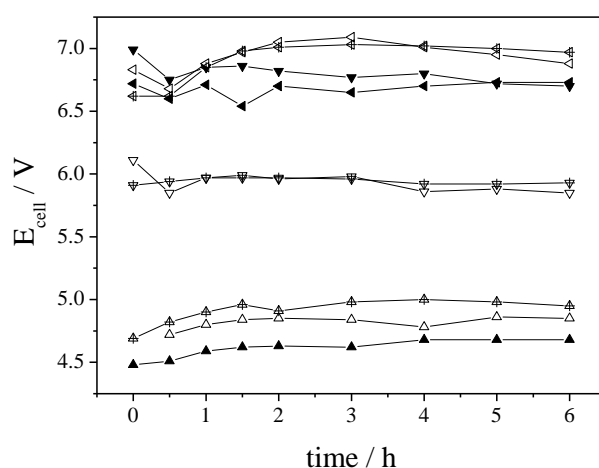


Figure 5 shows the initial pH and its variation during the electrolyses. For acidic solutions, the pH values are between 0.4 and 0.8, remaining practically constant throughout the electrolyses. Likewise, the pH for  $\text{Na}_2\text{CO}_3$  solutions remained in the range of 10-11.5, probably due to the buffer effect of this type of solution. However, for  $\text{Na}_2\text{SO}_4$ , the pH had a large variation during the phenol electrolysis, especially when  $\text{Cl}^-$  was present in the supporting electrolyte. This pH increase can be attributed to the unbalanced  $\text{OH}^-$  and  $\text{H}^+$  formation due to hydrogen evolution reaction (HER) and OER occurring at the cathode and anode, respectively.

The best values of reaction rates attained using chloride ions in acidic electrolytes can be explained by the formation of hypochlorous acid according to equation (3). This powerful oxidant contributes for the mediated oxidation of the organic compound.  $\text{HOCl}$  has an oxidizing power greater than that of hypochlorite, which is formed at pHs between 6 and 11 (equation (6)), which correspond to the pH values observed using  $\text{Na}_2\text{CO}_3$  and  $\text{Na}_2\text{SO}_4$  electrolytes. Therefore, fast oxidation rates were attained at low pH. In cases where  $\text{Cl}^-$  were used, the main importance of the type of supporting electrolyte is to achieve the best pH in which more oxidant chloro species and their concentrations can be obtained.

It is also interesting to notice in Figure 3(d) that phenolic compounds can be easier oxidized in the presence of chloride ions, indicating that the aromatic ring can react with chlorine species at pHs lower than  $\sim 9$ , which is that one obtained after approximately 2.5 hours of electrolysis using sodium sulfate, according to Figure 5(b). Using sodium carbonate, the pH values are greater than 10 and practically no influence of chloride ions on the TPC removal was observed.

### 3.3. Current efficiency and energy consumption.



**Figure 6.** Cell potential against time: ▲  $\text{H}_2\text{SO}_4$  in absence of  $\text{Cl}^-$  [ $42.7 \text{ mS cm}^{-1}$ ]; △  $\text{H}_2\text{SO}_4 + 200 \text{ mg L}^{-1} \text{ Cl}^-$  [ $45.3 \text{ mS cm}^{-1}$ ]; ⊞  $\text{H}_2\text{SO}_4 + 700 \text{ mg L}^{-1} \text{ Cl}^-$  [ $45.5 \text{ mS cm}^{-1}$ ]; ▼  $\text{Na}_2\text{CO}_3$  in absence of  $\text{Cl}^-$  [ $11.8 \text{ mS cm}^{-1}$ ]; ▽  $\text{Na}_2\text{CO}_3 + 200 \text{ mg L}^{-1} \text{ Cl}^-$  [ $11.8 \text{ mS cm}^{-1}$ ]; ⊚  $\text{Na}_2\text{CO}_3 + 700 \text{ mg L}^{-1} \text{ Cl}^-$  [ $11.4 \text{ mS cm}^{-1}$ ]; ◄  $\text{Na}_2\text{SO}_4$  in absence of  $\text{Cl}^-$  [ $16.4 \text{ mS cm}^{-1}$ ]; ◄  $\text{Na}_2\text{SO}_4 + 200 \text{ mg L}^{-1} \text{ Cl}^-$  [ $15.7 \text{ mS cm}^{-1}$ ]; ⊞  $\text{Na}_2\text{SO}_4 + 700 \text{ mg L}^{-1} \text{ Cl}^-$  [ $16.8 \text{ mS cm}^{-1}$ ]. Supporting electrolyte concentration =  $0.1 \text{ mol L}^{-1}$ . Electrolyte conductivities are shown in brackets.

Figure 6 shows the cell potential against time for the electrolytes studied in the absence and presence of chloride ions. According to equation (17),  $E_{\text{cell}}$  must be minimized in order to obtain low values of energy consumption. In general, it can be observed that there is a small  $E_{\text{cell}}$  variation at the beginning of the electrolyses then they remain approximately constant throughout the electrolysis. The only exception was for nitric acid, in which there was a huge increase of  $E_{\text{cell}}$  ( $\sim 2$  V), despite its highest conductivity ( $50 \text{ mS cm}^{-1}$ ), indicating that a passivating process on the electrode surface is occurring, probably due to some intermediate formed during the electrolysis.

It can be found in Figure 6 that low values of  $E_{\text{cell}}$  were obtained using sulfuric acid as supporting electrolyte due to its high conductivity. Nevertheless, it is interesting to notice that when sodium chloride is added, there was an increase of  $E_{\text{cell}}$ , despite the small conductivity enhancement. On the other hand, using carbonate electrolytes, the addition of  $200 \text{ mg L}^{-1}$  or  $700 \text{ mg L}^{-1} \text{ Cl}^{-}$  lead to a huge decrease of cell potential ( $\sim 0.8$  V). These results indicate that the addition of chloride ions creates an additional resistance that cannot be explained only by the IR drop. In the case of sodium carbonate electrolyte, a possible explanation would be inhibition of polymer passivation films formation on the electrode surface, which could occur at current and pH conditions used [25].

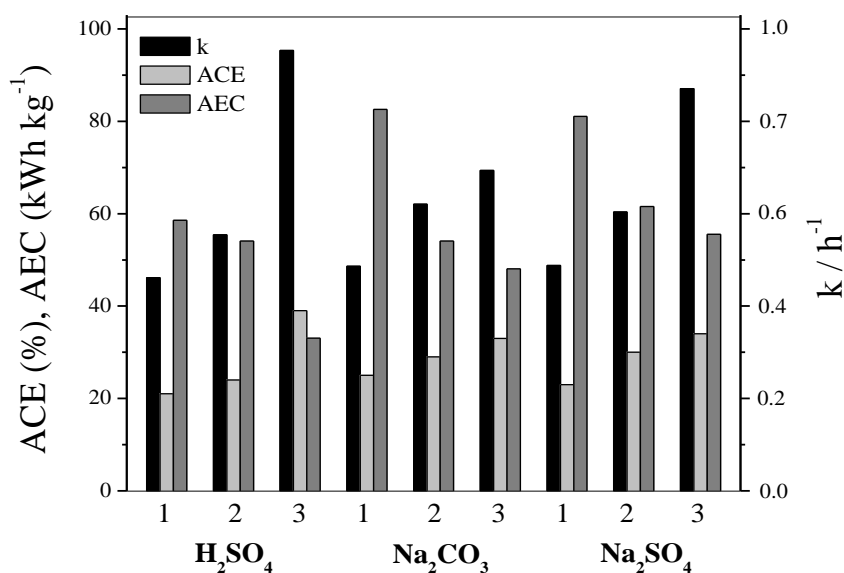


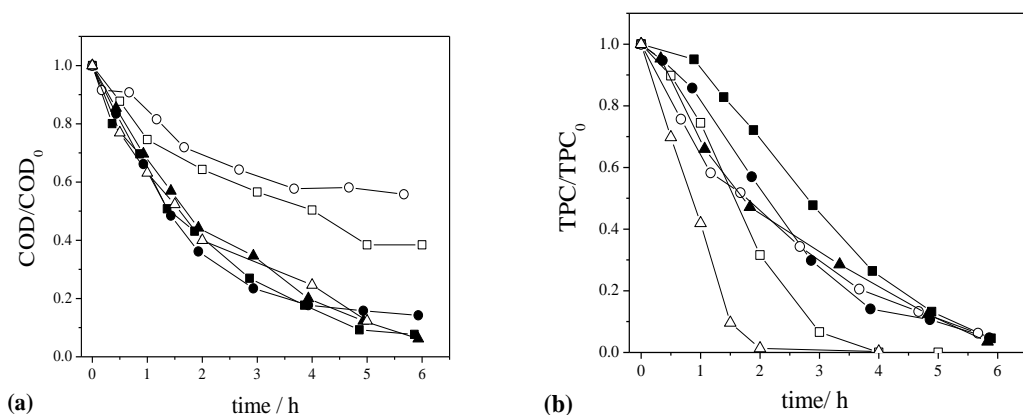
**Figure 7.** ACE, AEC, and  $k$  for the oxidation process carried out using different supporting electrolytes. 1 – absence of  $\text{Cl}^{-}$ , 2 –  $200 \text{ mg L}^{-1} \text{ Cl}^{-}$ ,  $700 \text{ mg L}^{-1} \text{ Cl}^{-}$ .

Although the ACE values for nitrate-containing electrolytes were not very different (13% and 15% for  $\text{HNO}_3$  and  $\text{Na}_2\text{SO}_4$ , respectively), their average energy consumption were high ( $90 \text{ kWh kg}^{-1}$  and  $140 \text{ kWh kg}^{-1}$  for  $\text{HNO}_3$  and  $\text{Na}_2\text{SO}_4$ , respectively); hence, in this case,  $E_{\text{cell}}$  was the major factor affecting the AEC. In the case of  $\text{H}_3\text{PO}_4$ , the AEC was slightly greater than those obtained using  $\text{H}_2\text{SO}_4$ ,  $\text{Na}_2\text{CO}_3$ , and  $\text{Na}_2\text{SO}_4$ , mainly due to its higher ACE. Zhu *et al.* [26] studied the degradation of phenol in a pilot-scale electrochemical reactor using sodium sulfate as supporting electrolyte. At optimized conditions, they obtained an energy consumption of  $31 \text{ kWh kg}^{-1}$  in the absence of chloride and applying a very low current density ( $8.5 \text{ mA cm}^{-2}$ ).

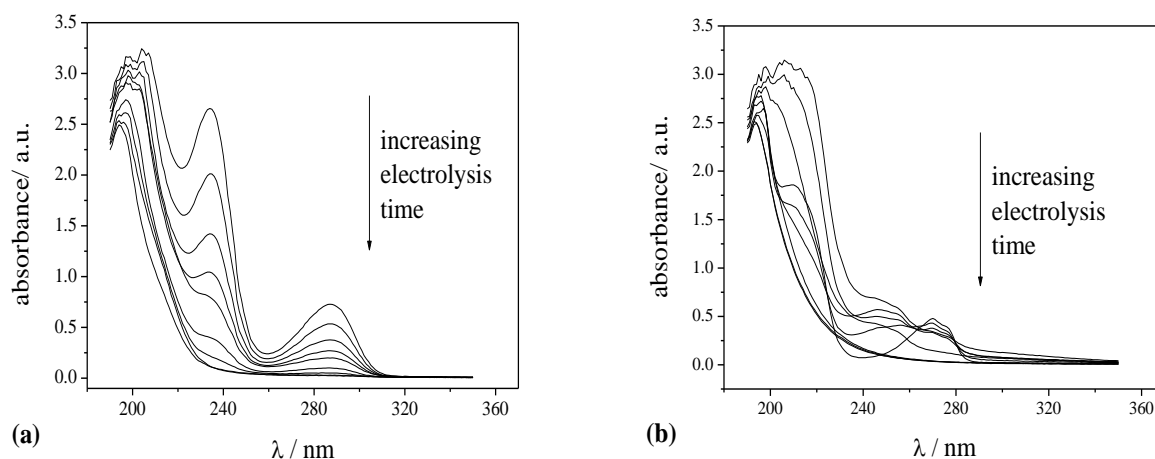
Figure 7 shows a comparison between the rate constant ( $k$ ), ACE, and AEC obtained using the supporting electrolytes in the presence and absence of  $\text{Cl}^-$ . The low values of ACE are due to the low phenol concentration that makes the process mass transfer controlled. As can be observed, the increase of reaction rates attained adding  $\text{Cl}^-$  greatly improves the ACE, leading to low values of AEC. This rule is especially important when sulfate-containing electrolytes were used.

It was found that for sulfate-containing electrolytes, the AEC cannot be improved by  $E_{\text{cell}}$  reduction when  $\text{Cl}^-$  is added, at least using the concentrations used in this work. Hence, the enhancement of reaction kinetics obtained using  $\text{Cl}^-$  was the main reason for the increase of ACE and, consequently, by the low values of AEC. In the case of sodium carbonate electrolytes, ACE and AEC improvements are due to both,  $E_{\text{cell}}$  reduction and kinetics enhancement. Considering these results, it seems that increasing the supporting electrolyte concentration, *i.e.*, increasing the ionic strength, could be an interesting alternative to improve the electrooxidation process.

### 3.4. Effect of ionic strength on process kinetics



**Figure 8.** Normalized COD (a) and TPC (b) against time. ■ H<sub>2</sub>SO<sub>4</sub>, I = 0.3 mol L<sup>-1</sup>; □ H<sub>2</sub>SO<sub>4</sub>, I = 3.0 mol L<sup>-1</sup>; ● Na<sub>2</sub>CO<sub>3</sub>, I = 0.3 mol L<sup>-1</sup>; ○ Na<sub>2</sub>CO<sub>3</sub>, I = 3.0 mol L<sup>-1</sup>; ▲ Na<sub>2</sub>SO<sub>4</sub>, I = 0.3 mol L<sup>-1</sup>; △ Na<sub>2</sub>SO<sub>4</sub>, I = 3.0 mol L<sup>-1</sup>. COD<sub>0</sub> = 666 mg L<sup>-1</sup> (280 mg L<sup>-1</sup> phenol), TPC<sub>0</sub> = 30 mg L<sup>-1</sup> gallic acid



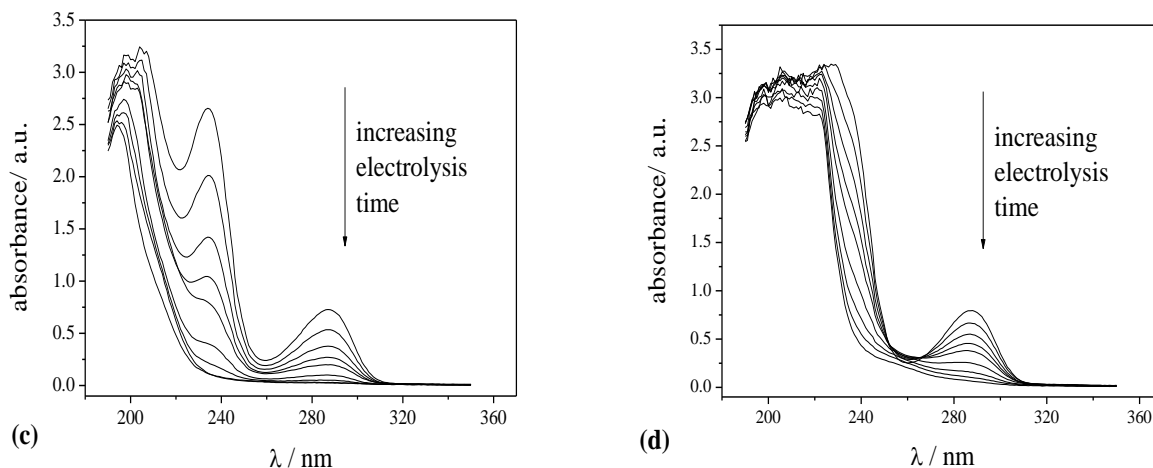


**Figure 9.** UV spectra for the supporting electrolytes along the electrolysis. (a)  $\text{H}_2\text{SO}_4$ ,  $0.3 \text{ mol L}^{-1}$ ; (b)  $\text{H}_2\text{SO}_4$ ,  $3.0 \text{ mol L}^{-1}$ ; (c)  $\text{Na}_2\text{CO}_3$ ,  $0.3 \text{ mol L}^{-1}$ ; (d)  $\text{Na}_2\text{CO}_3$ ,  $3.0 \text{ mol L}^{-1}$ .

Figure 8 shows the results of normalized COD and TPC against time obtained using  $\text{H}_2\text{SO}_4$ ,  $\text{Na}_2\text{CO}_3$  and  $\text{Na}_2\text{SO}_4$  with different ionic strengths, in the absence of  $\text{Cl}^-$ . As can be seen in Figure 8(a), using  $\text{Na}_2\text{SO}_4$  the difference in COD removal rates was not significant when the ionic strength was increased from  $0.3$  to  $3.0 \text{ mol L}^{-1}$ . On the other hand, for  $\text{H}_2\text{SO}_4$  and  $\text{Na}_2\text{CO}_3$  electrolytes, the ionic strength had a strong influence on the COD-time curves. In these cases, there was a COD reduction during the few first hours of electrolysis and afterwards, it stopped. These experiments were replicated, but identical results were obtained. A possible explanation would be the competition between organic molecules and anions by the active electrode sites [27]. In the case of sulfuric acid, the high sulfate concentration at low pH could favor the formation of persulfuric acid, which is quite unstable in solution, decomposing back to sulfuric acid, thus interfering in the COD measurement [28]. In the case of sodium carbonate, interferences on COD measurement at high carbonate concentrations could also explain the results. The assumption of COD interference appears to be more consistent with the results of UV absorbance shown in Figure 9, where it can be observed that using  $I = 3.0 \text{ mol L}^{-1}$   $\text{H}_2\text{SO}_4$ , despite the occurrence of a new absorption band at  $\sim 250 \text{ nm}$  (which can be attributed to an intermediate), the solution spectra after 5 or 6 hours of electrolysis were quite similar to those obtained using  $I = 0.3 \text{ mol L}^{-1}$   $\text{H}_2\text{SO}_4$ . The same conclusions can also be drawn regarding to  $\text{Na}_2\text{CO}_3$ . For  $\text{Na}_2\text{SO}_4$  electrolytes there were no significant differences in the spectra obtained using the two different ionic strengths. It is also interesting to notice in Figure 9 that the reduction of phenol absorbance band at approximately  $280 \text{ nm}$  corroborates the results of TPC removal shown in Figure 8(b), where it can be observed that the TPC removal is greatly improved using sodium sulfate electrolytes, thus in agreement with other authors [13,29].

The cell potentials obtained using  $I = 3.0 \text{ mol L}^{-1}$  remained practically constant throughout the electrolyses, but the values of the average cell potential decreased  $0.7 \text{ V}$  and  $2.5 \text{ V}$  when the ionic strength was increased adding more  $\text{H}_2\text{SO}_4$  and  $\text{Na}_2\text{CO}_3$ , respectively. Table 1 shows the comparison of the electrolyte conductivity, average cell potential ( $E_{\text{cell,av}}$ ), ACE, and AEC for the process carried out using  $0.3$  and  $3.0 \text{ mol L}^{-1}$ .

Considering that apparently was not possible to remove all COD using  $\text{H}_2\text{SO}_4$  and  $\text{Na}_2\text{CO}_3$  with  $I = 3.0 \text{ mol L}^{-1}$ , their effect on energy consumption could not be evaluated. On the other hand, the increase of electrolyte conductivity obtained using high  $\text{Na}_2\text{SO}_4$  concentration did not have any influence on the cell potential, thus the small increase of AEC can be attributed to a small decrease on current efficiency. Regarding to the pH, except for the  $\text{Na}_2\text{SO}_4$  electrolyte, it remained practically constant throughout the experiment for electrolytes containing  $\text{H}_2\text{SO}_4$  (1.08 for  $I = 0.3 \text{ mol L}^{-1}$ ) and  $\text{Na}_2\text{CO}_3$  (10.7 and 11.6 for  $I = 0.3 \text{ mol L}^{-1}$  and  $3.0 \text{ mol L}^{-1}$ , respectively). Using  $\text{Na}_2\text{SO}_4$  the initial pH was 5.0 for both ionic strength and reached the values of 6.5 and 12.5 at the end of the electrolyses, for  $I = 0.3 \text{ mol L}^{-1}$  and  $3.0 \text{ mol L}^{-1}$ , respectively.

**Table 1.** Conductivity, average cell potential, ACE, and AEC

Supporting electrolyte	$\sigma / \text{mS cm}^{-1}$	$E_{\text{cell, av.}} / \text{V}$	ACE* / %	AEC* / $\text{kWh kg}^{-1}$
$\text{H}_2\text{SO}_4$ , $I = 0.3 \text{ mol L}^{-1}$	42.7	4.6	21.5	57
$\text{H}_2\text{SO}_4$ , $I = 3.0 \text{ mol L}^{-1}$	455	3.9	-	-
$\text{Na}_2\text{CO}_3$ , $I = 0.3 \text{ mol L}^{-1}$	11.8	6.8	21.9	84
$\text{Na}_2\text{CO}_3$ , $I = 3.0 \text{ mol L}^{-1}$	82.6	4.3	-	-
$\text{Na}_2\text{SO}_4$ , $I = 0.3 \text{ mol L}^{-1}$	16.4	6.7	20.5	92
$\text{Na}_2\text{SO}_4$ , $I = 3.0 \text{ mol L}^{-1}$	92.0	6.7	19.5	103

Although the best result in terms of AEC was obtained using  $\text{H}_2\text{SO}_4$  electrolytes in the presence of  $700 \text{ mg L}^{-1} \text{ Cl}^-$ , the cost of an eventual effluent acidification and neutralization would not be justified. The use of low concentrations ( $0.1 \text{ mol L}^{-1}$ ) of sodium sulfate or sodium carbonate would be the best options to achieve high effluent conductivity and fast reaction rates. Furthermore, the addition of  $\text{Cl}^-$  can reduce AEC by increasing ACE. Using  $\text{Na}_2\text{CO}_3$  or  $\text{Na}_2\text{SO}_4$  containing  $700 \text{ mg L}^{-1} \text{ Cl}^-$ , an ACE reduction of 45% and 55% can be obtained, respectively. A further reduction of AEC is supposed to be obtained using chloride concentrations higher than  $700 \text{ mg L}^{-1}$ , but there is a limit, as pointed by several authors [19,30].

#### 4. CONCLUSION

In this work we studied the effect of different acids and sodium salts as supporting electrolytes for phenol electrooxidation in the absence and presence of chloride ions. It was found that nitrate electrolytes showed the worst performance for COD removal. The oxidation kinetics constants for the other supporting electrolytes studied followed the order  $k_{\text{Na}_2\text{SO}_4} \approx k_{\text{Na}_2\text{CO}_3} > k_{\text{H}_2\text{SO}_4} > k_{\text{H}_3\text{PO}_4}$ . When chloride ions is added, there is a huge increase of the reaction kinetics and a new order is established:  $k_{\text{H}_2\text{SO}_4} > k_{\text{Na}_2\text{SO}_4} > k_{\text{Na}_2\text{CO}_3}$ . The best kinetics constants obtained using acid solutions can be explained

by the mediated oxidation through the more oxidative chloro species formed at low pH values. Although, the higher the chloride concentration the faster the reaction kinetics, any process improvement was observed by increasing the supporting electrolyte concentration. In conclusion, the electrooxidation process is much more sensitive to the presence of chloride than to the formation of peroxydisulfate or peroxy carbonate by using sulfate and carbonate electrolytes, respectively. Regarding to the average current efficiency and energy consumption, the best values were obtained using sulfuric acid and chloride ions, not only due to the kinetic improvement, but also due to the low  $E_{\text{cell}}$  value which is a consequence of the high solution conductivity.

#### ACKNOWLEDGEMENTS

Fundação de Amparo à Pesquisa do Estado de São Paulo - FAPESP (2009/15361-3) is acknowledged for the financial support. Renata B. A. Souza thanks CAPES (Coordenação de Aperfeiçoamento de Pessoal de Nível Superior) for the fellowship.

#### References

1. C. Bayer, M. Follmann, T. M. Wintgens, K. Larsson, M. Almemark, *Water Sci Technol*, 62 (2010) 915.
2. A. Anglada, A. Urtiaga, I. Ortiz, *J Chem Technol Biotechnol*, 84 (2009) 1747.
3. L.A.M. Ruotolo, J. C. Gubulin, *Chem Eng J*, 149 (2009) 334.
4. C. Borrás, C. Berzoy, J. Mostany, J. C. Herrera, B. R. Scharifker, *Appl Catal B-Environ*, 72 (2007) 98.
5. L. S. Andrade L.S., R. C. Rocha-Filho, N. Bocchi, S. R. Biaggio, J. Iniesta, V. Garcia-Garcia, V. Montiel, *J Hazard Mater*, 153 (2008) 252.
6. E. Weiss, K. Groenen-Serrano, A. A. Savall, *J Appl Electrochem*, 38 (2008) 329.
7. J. R. Sun., H. Lu, H. B. Lin, L. L. Du, W. M. Huang, H. D. Li, T. Cui, *Sep Purif Technol*, 88 (2012) 116.
8. C. A. Martinez-Huitle, S. Ferro, *Chem Soc Rev*, 35 (2006) 1324.
9. R. D. Coteiro, A. R. De Andrade, *J Appl Electrochem*, 37 (2007) 691.
10. I. D. Santos, J. C. Afonso, A. J. B. Dutra, *Sep Purif Technol*, 76 (2010) 151.
11. C. Y. Cheng, G. H. Kelsall, *J Appl Electrochem*, 37 (2007) 1203.
12. M. E. H. Bergmann, J. Rollin, *Catal Today*, 124 (2007) 198.
13. P. Cañizares, J. Lobato, R. Paz, M. A. Rodrigo, C. Sáez, *Water Res*, 39 (2005) 2687.
14. P. Cañizares, C. Sáez, A. Sanchez-Carretero, M. A. Rodrigo, *J Appl Electrochem*, 39 (2009) 2143.
15. P. Cañizares, J. Garcia-Gomes, C. Sáez, M. A. Rodrigo, *J Appl Electrochem*, 34 (2004) 87.
16. L. S. Andrade, L. A. M. Ruotolo, R. C. Rocha-Filho, N. Bocchi, S. R. Biaggio, J. Iniesta, V. Garcia-Garcia, V. Montiel, *Chemosphere*, 66 (2007) 2035.
17. C. Cominellis, G. Chen, *Electrochemistry for the Environment*, Springer, New York (2010).
18. J. M. Aquino, M. A. Rodrigo, R. C. Rocha-Filho, C. Sáez, P. Cañizares, *Chem Eng J*, 184 (2012) 221.
19. M. S. Saha, T. Furuta, Y. Nishiki, *Electrochem Commun*, 6 (2004) 201.
20. V. L. Singleton, R. Orthofer, R. M. Lamuela-Raventos, *Method Enzymol*, 299 (1999) 152.
21. A. M. Polcaro, A. Vacca, M. Mascia, F. Ferrara, *J Appl Electrochem* 38 (2008) 979.
22. S. Malato, J. Blanco, C. Richter, B. Milow, M. I. Maldonado, *Chemosphere*, 38 (1999) 1145.
23. P. Patnaik, J. N. Khoury, *Water Res*, 38 (2004) 206.

24. M. Li, F. Chuanping, Z. Zhang, X. Lei, R. Chen, Y. Yang, N. Sugiura, *J Hazard Mater*, 171 (2009) 724.
25. N.B. Tahar, A. Savall, *J Appl Electrochem*, 41 (2011) 983.
26. X. Zhu, J. Ni, J. Wei, X. Xing, H. Li, Y. Jiang, *J. Hazard Mater*, 184 (2010) 493.
27. I. M. Kolthoff, I. K. Miller, *J Am Chem Soc*, 73 (1951) 3055.
28. S. M. L. Agostinho, R. F. V. Villamil, A. A. Neto, H. O. Aranha, *Quim Nova*, 27 (2004) 813.
29. P. H. Britto-Costa, L. A. M. Ruotolo, *Braz J Chem Eng* (2012), in press.
30. S. A. Neto, A. R. De Andrade, *Electrochim Acta*, 54 (2009) 2039.